

Theoretical Characterization of Charge Transport in One-Dimensional Collinear Arrays of Organic Conjugated Molecules

Lucas Viani,^[a] Yoann Olivier,^[a] Stavros Athanasopoulos,^[a] Demetrio A. da Silva Filho,^[b] Jürg Hulliger,^[c] Jean-Luc Brédas,^[a, b] Johannes Gierschner,^[a, d] and Jérôme Cornil^{*[a, b]}

A great deal of interest has recently focused on host–guest systems consisting of one-dimensional collinear arrays of conjugated molecules encapsulated in the channels of organic or inorganic matrices. Such architectures allow for controlled charge and energy migration processes between the interacting guest molecules and are thus attractive in the field of organic electronics. In this context, we characterize here at a quantum-chemical level the molecular parameters governing charge transport in the hopping regime in 1D arrays built with

different types of molecules. We investigate the influence of several parameters (such as the symmetry of the molecule, the presence of terminal substituents, and the molecular size) and define on that basis the molecular features required to maximize the charge carrier mobility within the channels. In particular, we demonstrate that a strong localization of the molecular orbitals in push–pull compounds is generally detrimental to the charge transport properties.

1. Introduction

Crystalline organic materials such as perhydrotriphenylene (PHTP) and tris(*o*-phenylenedioxy)cyclotriphosphazene (TPP) or inorganic mesoporous materials such as zeolite L feature narrow one-dimensional (1D) channels in which electroactive dyes can be incorporated to form a supramolecular organization of the guest molecules confined in one dimension (Figure 1a).^[1–6] Such host–guest systems are currently studied for the development of tailored photo- and electro-responsive hybrid systems, in particular for solar cell applications.^[1–11] The incorporation of the molecules within the channels allows for a strong reduction of interchain interaction effects and can thus

significantly improve the light emission properties of the molecules.^[7–9] A large variety of neutral and cationic dyes have been inserted in such channels^[1–4, 6, 12, 13] and relevant information such as the structural dynamics^[11, 14] and photophysical properties of the host–guest compounds have been characterized at the experimental and theoretical level.^[6, 15–18] Host–guest systems are also ideal candidates to study key processes such as energy migration and charge transport along or between the channels. Energy transport in such systems has been the topic of many recent experimental and theoretical papers;^[4, 6, 12, 19–21] the migration of excitations can occur both along and between the channels^[4, 12] and has thus generally a three-dimensional character.

In contrast, the potential of regular one-dimensional arrays of conjugated molecules to efficiently transport charges over long distances has received much less attention.^[22] Electronic

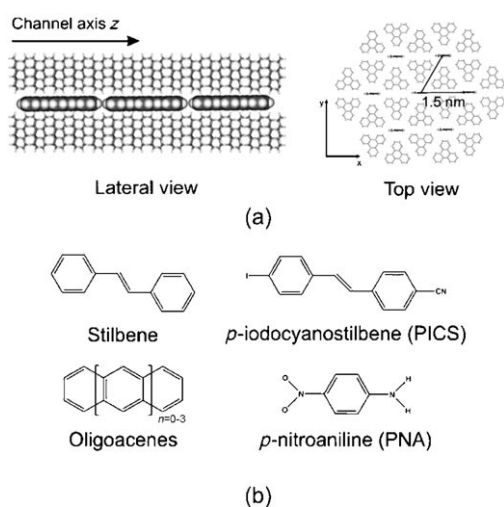


Figure 1. a) Schematic representation of a PHTP host–guest system with collinear guest molecules in the channel; b) Molecular structure of the compounds.

[a] L. Viani, Dr. Y. Olivier, Dr. S. Athanasopoulos, Prof. Dr. J.-L. Brédas, Dr. J. Gierschner, Dr. J. Cornil
Laboratory for Chemistry of Novel Materials
University of Mons, Place du Parc 20, B-7000 Mons (Belgium)
Fax: (+ 32) 65373861
E-mail: jerome@averell.umh.ac.be

[b] Dr. D. A. da Silva Filho, Prof. Dr. J.-L. Brédas, Dr. J. Cornil
School of Chemistry and Biochemistry and
Center for Organic Photonics and Electronics
Georgia Institute of Technology, Atlanta, Georgia 30332-0400 (USA)

[c] Prof. Dr. J. Hulliger
Department of Chemistry and Biochemistry
University of Berne, Freiestrasse 3, CH-3012 Berne (Switzerland)

[d] Dr. J. Gierschner
Madrid Institute of Advanced Studies (IMDEA-Nanoscience)
UAM, Faculty of Science, Module C-IX, 3rd Level
Av. Tomás y Valiente, 7 Campus Cantoblanco, E-28049 Madrid (Spain)

coupling between molecules in adjacent channels is negligible due to the exponential distance dependence,^[23] which promotes pure 1D charge transport characteristics. This also implies that a full, defect-free loading of the channels is required to transport charges along them. Most of the presently known channel-forming host materials are not suited to achieve dense packing, since many systems such as zeolite L do not offer a homogeneous environment for the incorporated molecules; these materials provide preferential sites inside the channels and prevent close contacts between the guest molecules. A good candidate for close intra-channel guest–guest contacts is PHTP, where the inner surface of the channels is made of aliphatic hydrogen atoms. In this case, a smooth and weakly interacting hydrophobic channel surface is created and prevents the occurrence of preferential locations for the guest molecules. The small diameter of the channel (about 5 Å) requires the insertion of rod-shaped guest molecules and forces them to be in a strict collinear 1D arrangement, with a large separation (15 Å) between supramolecular wires. Moreover, the tight channel walls allow only for limited (dynamic) deviation from the 1D collinear arrangement^[11,14] and thus keep energetic/positional disorder small in the channels.^[6] The 1D character of electronic transport is clearly seen from photoconductivity measurements that yield a current perpendicular to the channel axis hundred times lower than along the molecular chains.^[22]

In order to assess the potential of guest molecules inserted into PHTP-like matrices, we characterize here at a quantum-chemical level 1D charge transport along collinear arrays made of different types of molecules in order to determine the molecular features required to maximize charge transport. For this purpose, we investigate the influence of several factors, such as the symmetry of the molecule, the nature of substituents, and the molecular size, on the transport parameters. Our selection, depicted in Figure 1b, encompasses: i) *para*-nitroaniline (PNA), a small prototypical non-centrosymmetric push–pull compound; ii) the neutral centrosymmetric stilbene molecule versus the non-centrosymmetric *para*-iodocycano stilbene derivative (PICS); and iii) oligoacenes ranging from 2 to 5 rings to analyze the impact of increasing the delocalization length. Note that among the selected molecules, stilbene, naphthalene, and anthracene have been inserted into zeolite channels,^[2] stilbene into PHTP,^[6] and PNA into TPP.^[3]

2. Theoretical Background

Since the molecules interact only via their terminal ends, charge transport along the channels is expected to operate in a weak coupling regime, namely with hopping processes in which localized charges (polarons) jump from molecule to molecule. In this regime, the charge transfer rate between two adjacent units can be estimated in the framework of the Marcus–Levich–Jortner formalism as Equation (1):^[24,25]

$$k_{\text{hop}} = \frac{2\pi}{\hbar} t^2 \frac{1}{\sqrt{4\pi\lambda_s k_B T}} \sum_{\nu} e^{-S} \frac{S^{\nu}}{\nu!} e^{-\frac{(\Delta G^{\circ} + \lambda_s + \nu\hbar\omega)^2}{4\pi\lambda_s k_B T}} \quad (1)$$

where t is the transfer integral between the electronic levels in interaction, ν the vibrational quantum number in the final state, $\hbar\omega$ the energy of an effective intramolecular mode assisting the transfer treated explicitly at a quantum-mechanical level (a value of 0.2 eV typical for stretching modes in organic molecules has been chosen here), ΔG° the free enthalpy of the reaction, λ_s the external reorganization energy, and S the Huang–Rhys factor directly related to the internal reorganization energy λ_i ($S = \lambda_i/\hbar\omega$). The charge localization expected in the hopping regime occurs when electronic couplings (transfer integrals) are much smaller than the total reorganization energy, as it is the case for the systems under study (vide infra); the localization is further reinforced in actual systems by the influence of lattice dynamics.^[26]

Transfer integrals are commonly estimated as half the splitting of the highest occupied (HOMO) and lowest unoccupied (LUMO) molecular orbitals for hole and electron transport, respectively.^[27] However, this approach is often biased by polarization effects which create in non-centrosymmetric structures an initial offset of the electronic levels before they start interacting; such an offset does not contribute to the transfer efficiency.^[28,29] Thus, site energies, ε_1 and ε_2 , and transfer integrals, t_{12} , should be obtained directly from the matrix elements given in Equation (2):

$$\begin{aligned} \varepsilon_i &= \langle \psi_i | H | \psi_i \rangle \\ t_{ij} &= \langle \psi_i | H | \psi_j \rangle \end{aligned} \quad (2)$$

with H the one-electron Hamiltonian of the system and ψ the HOMO or LUMO of the individual units. Along the line of recent theoretical works,^[28,30] the transfer integral values have been calculated in a direct way within a fragment approach at the density functional theory (DFT) level using the B3LYP functional with a triple zeta polarized (TZP) basis set, as implemented in the Amsterdam density functional (ADF) package. In this approach, the orbitals of the dimer are expressed as a linear combination of the molecular orbitals of the individual units (i.e. fragments) that are obtained by solving the Kohn–Sham equations. Since the fragment orbitals form a non-orthogonal basis set, the transfer integrals depend on the choice of the energy origin;^[31] the addition of a constant G to the initial electronic Hamiltonian leads to a shift of the transfer integral value by an amount equal to the product of G and the orbital overlap S_{12} , so that the transfer integral is no longer an invariant.^[32] The problem can be solved by calculating the parameter with an orthogonal basis set by applying the Löwdin transformation ($H = S^{-1/2} H S^{-1/2}$) to the initial electronic Hamiltonian. In this framework, the invariant transfer integral (\tilde{t}_{12}) involved in Equation (1) is evaluated via Equation (3):

$$\tilde{t}_{12} = \frac{t_{12} - \frac{1}{2}(\varepsilon_1 + \varepsilon_2)S_{12}}{1 - S_{12}^2} \quad (3)$$

The total reorganization energy λ is another important parameter built from two different contributions: an internal part λ_i that reflects the changes in the geometry of the two molecules during the transfer^[27] and an external part λ_s describing

the nuclear displacements in the surrounding medium and the resulting changes in electronic polarization energies.^[24] Since λ_s primarily depends on the nature of the environment, we have assumed as a first approximation that this parameter is the same for all compounds for a given host; since there is no simple approach to compute this parameter, λ_s has been considered here as a tunable parameter and has been set to reasonable values of 0.2 eV or 0.3 eV^[33] to simulate changes in the flexibility and polarizability of the host. The λ_i values (and hence the Huang–Rhys factors) have been calculated at the DFT level using the B3LYP functional and a 6-311G** basis set, as described earlier.^[27] For oligoacenes, this approach yields a good quantitative agreement between the theoretical estimates and the experimental values extracted from gas-phase ultraviolet photoelectron spectra (UPS).^[34]

In a simple one-electron picture, the Gibbs free energy ΔG^0 associated to the charge transfer corresponds to the energy difference between the HOMO or LUMO levels of the two molecules. This energy difference can be induced by changes in the nature of the environment, application of an external electric field that creates an energy gradient of the levels,^[35] or electrostatic interactions between the molecules, especially in the case of push–pull compounds due to the presence of a permanent dipole moment.^[36]

On the basis of these parameters, the transfer rates can be estimated from Equation (1). The charge mobility μ was then estimated using Equation (4) for a frozen regular array of molecules:^[37]

$$\mu = \frac{ea^2}{k_B T} k_{\text{hop}} \quad (4)$$

with e the electronic charge, a the separation between the centers of mass of two adjacent molecules, k_B the Boltzmann constant, and k_{hop} the hopping rate provided by Equation (1). The use of Equation (4) is expected to provide an upper limit of the mobility value due to the neglect of static conformational disorder. However, such a disorder is expected to be considerably reduced in PHTP-like matrices since: i) the tight cavity walls hinder possible rotations of the molecules in the channels;^[11,14] and ii) the inert character of the walls promotes stronger guest–guest contacts and hence a weak distribution of intermolecular distances keeping the molecules in van der Waals contacts.^[6] Moreover, such distributions are known to weakly impact mobility values due to compensation effects between jumps at shorter versus longer distances compared to the average value.^[35] In the next section, we describe the variations in the transfer integrals among the different compounds before estimating the expected range of charge mobility values.

3. Results and Discussion

3.1. Transfer Integrals

In order to gauge the efficiency of charge transfer between molecules aligned within a narrow channel, we have first com-

puted the transfer integrals for holes between two stilbene molecules in a cofacial *versus* collinear configuration for various separations between the centers of mass of the two molecules (Figure 2). The transfer integrals are found to vary by two

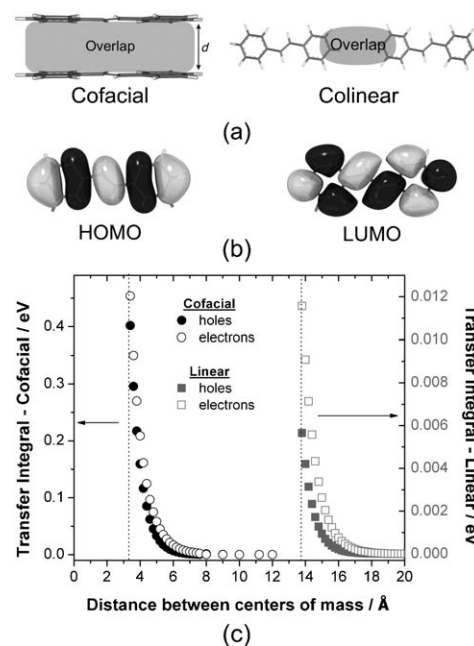


Figure 2. a) Illustration of the electronic overlap for a cofacial versus collinear arrangement of two stilbene molecules as a function of intermolecular separation (between the centers of mass); b) shape of the HOMO and LUMO levels of the stilbene molecule; c) computed transfer integrals for holes between two stilbene molecules in a cofacial *versus* collinear configuration for various separations between the centers of mass of the two molecules.

orders of magnitude between the two different arrangements, up to 400 meV for the closest contact distance of 3.4 Å in the cofacial geometry (as estimated from the van der Waals radii) and up to 5.6 meV for the closest contact distance of 13.8 Å (separation between the centers of mass) in the aligned geometry. This huge difference is rationalized by the large contact area between the two molecules in the cofacial geometry which promotes a strong interaction between the π -electron clouds of the two molecules; on the other hand, the reduced contact in the collinear dimer induces interactions only between the p_z atomic orbitals located on the terminal atoms. The splitting of the frontier orbitals decreases exponentially as a function of distance [Eq. (5)]:^[29]

$$t = t_0 \exp(-\beta d) \quad (5)$$

with β the decay factor (estimated here from Figure 2b to be on the order 1.5 \AA^{-1}) and d the separation between the centers of mass of the two molecules. Similar considerations apply for all compounds both for hole and electron transport. In the following, we will thus investigate whether the very low transfer integrals calculated for stilbene in the collinear geometry can be significantly increased by molecular design (i.e. by changing

the size of the molecule and/or introducing terminal electroactive substituents).

The chain-length dependence of the transfer integral both for holes and electrons has been examined for collinear oligoacenes containing from 2 to 5 rings in van der Waals contact. In both cases, the transfer integral decreases with an increase in the number of rings. This evolution is driven by the reduction in electronic density over the two terminal atoms due to the progressive delocalization of the electronic levels. The sum of the square of the LCAO coefficients associated to the p_z atomic orbital of the two terminal carbon atoms in pentacene is reduced by about 43% in the HOMO and LUMO levels when compared to naphthalene, as illustrated in Figure 3. Although

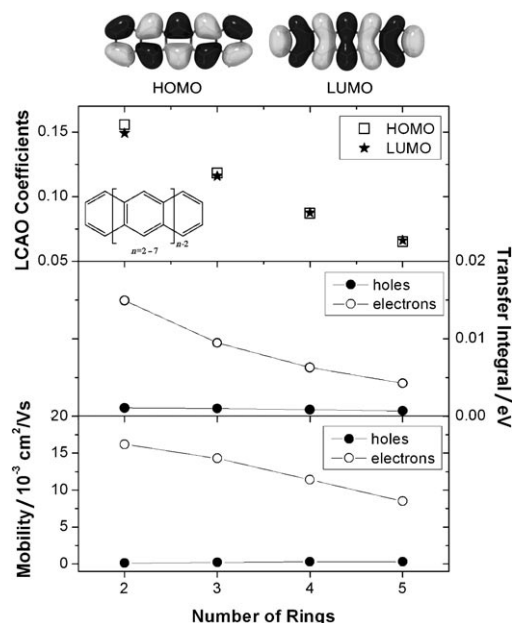


Figure 3. Evolution of the sum of the square of the LCAO coefficients over the two terminal carbon atoms (top) and the mobility (bottom) in collinear arrangement of oligoacenes in van der Waals contact as a function of the number of rings. The shape of the HOMO and LUMO levels of pentacene are displayed.

the sums of the square of the LCAO coefficients are almost equal in the HOMO and LUMO levels, transfer integrals for holes and electrons are of very different magnitude due to different degree of bonding versus antibonding interactions in the overlapping region.^[23] This is illustrated by the shapes of the HOMO and LUMO levels of pentacene showing that there is a bonding interaction between the p_z atomic orbitals on the terminal carbon atoms in the LUMO (translating into a large transfer integral value) while an antibonding character prevails in the HOMO (leading to a small transfer integral value as a result of compensation effects). These results indicate that transfer integrals can be maximized by the use of: i) *short molecular systems*; and ii) *systems with large LCAO coefficients on the terminal atoms in the frontier orbitals*. Note, however, that the actual mobility values in the oligoacene series will not be

only driven by the transfer integral (and hence the hopping rate) between two adjacent molecules but also by the number of jumps. We will come back to this issue in Section 3.2.

A molecule which might promote large transfer integral values is *para*-nitroaniline (PNA, see Figure 4), that is, a proto-

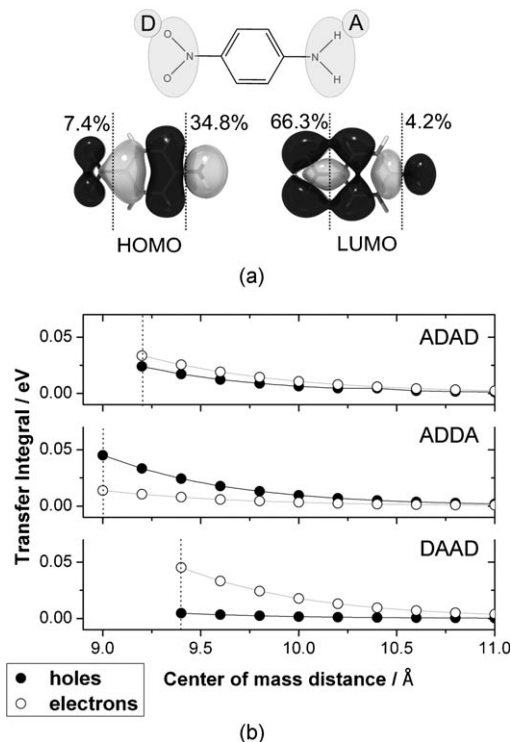


Figure 4. a) Shape of the HOMO and LUMO levels of PNA and distribution over the donor and acceptor parts based on the electronic density; b) evolution of the transfer integral as a function of the separation between the centers of mass for the DAAD, ADDA, and ADAD configurations; dashed lines point to the van der Waals contact distance.

type push-pull system bearing a short conjugated segment and terminal amino and nitro groups acting as π -donor (D) and π -acceptor (A) substituents. The latter are introduced to attract the electronic density around the terminal parts of the molecule. In PNA, the LUMO is strongly localized on the acceptor part (66.3% of the wavefunction resides over the nitro group when analyzing the electronic distribution) whereas the HOMO is more delocalized though being centered towards the donor part of the molecule. For a collinear arrangement of two PNA molecules, three different configurations can in principle be considered, namely ADAD, ADDA and DAAD. Note that the ADAD configuration is energetically favored due to the collinear alignment of the two permanent dipole moments. Figure 4b shows the dependence of the transfer integrals for holes and electrons in the three different configurations as a function of intermolecular separation, starting from the closest contact allowed by the van der Waals radii.

For the ADDA configuration, where the overlap between the HOMOs is stronger than between the LUMOs, the transfer integral does not exceed 45 meV for holes and is consistently

much smaller for electrons, see Figure 4b; the opposite situation is found for the DAAD configuration. This evolution is rationalized by the fact that the HOMO [LUMO] level is weakly localized over the acceptor [donor] part, thus yielding a small electronic overlap in the DAAD [ADDA] configuration. The situation appears to be intermediate in the case of the ADAD configuration. Thus, the energetically favored ADAD alignment generally expected within the channels offers the most attractive charge transport properties. Indeed, a molecular packing designed to be of ADDAADDA type would strongly reduce the hole or electron current density through the AA and DD connections, respectively. DAAD or ADDA connections appearing at the trace level in channels^[18] are thus expected to act as limiting steps for hole and electron transport, respectively. Good candidates for 1D charge transport should thus exhibit electroactive substituents bearing a significant electronic density over their terminal atoms; this suggests avoiding hydrogen atoms that do not participate in the description of the frontier electronic levels. Another constraint is to avoid highly localized frontier orbitals in the donor or acceptor moieties and to promote a dominant bonding (or antibonding) interaction in the overlapping region to maximize the transfer integral.^[23]

In order to optimize the end groups of stilbene according to these guidelines, we investigated *p*-iodo,*p*'-cyanostilbene (PICS, see Figure 1b) with terminal iodine (donor) and cyano (acceptor) moieties. Here, the HOMO level is delocalized over the

molecule and bears significant electron density on both the iodine and nitrogen atoms, see Figure 5a. In the ADAD arrangement (i.e. the most stable configuration in the channel due to dipole–dipole interactions), the transfer integral value is increased for holes by about a factor of three compared to stilbene (14.3 versus 5.6 meV, respectively); in turn, this increases the charge transfer rate by one order of magnitude, see Equation (1). The significant weight of the HOMO on the iodine atom yields significantly lower transfer integral in the DAAD configuration (3.8 meV) compared to ADDA (41.6 meV), see Figure 5b. In contrast, in the LUMO, the LCAO coefficient associated to iodine is smaller, which translates into more homogeneous values for the different arrangements, these are, values of 11.1, 11.6, and 9.1 meV in the ADAD, DAAD, and ADDA cases, respectively.

When replacing the cyano group by a nitro group, the transfer integrals in the DADA arrangement decrease down to 9.2 and 8.1 meV for holes and electrons, respectively; this can be mainly assigned to the smaller LCAO coefficients on the oxygen atoms. Slightly larger values (9.7 and 11.6 meV for holes and electrons, respectively) are obtained for the the *p*-iodo,*p*'-nitro-biphenyl molecule studied by Quintel and Hulliger in their experimental work.^[22] The shortening in the conjugation length when replacing stilbene with biphenyl is partly compensated here by a loss of conjugation due to the torsion between the phenyl rings.

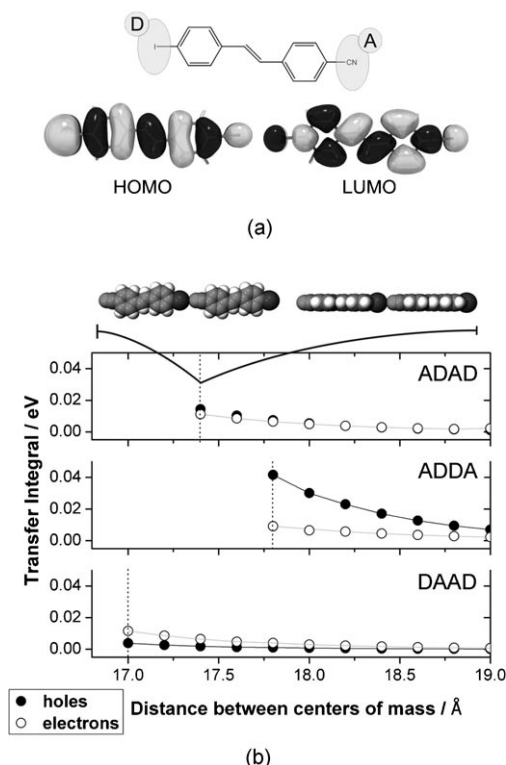


Figure 5. a) Shape of the HOMO and LUMO levels of PICS; b) evolution of the transfer integral as a function of the separation between the centers of mass for the DAAD, ADDA, and ADAD configurations; dashed lines point to the van der Waals contact distance, where the arrangement of the molecules is depicted.

3.2. Charge Mobility

Charge mobilities μ have been estimated from Equations (1) and (4) for a frozen 1D array of stilbene molecules and oligoacenes and for the energetically favored ADAD configuration of the PNA and PICS molecules; these values are expected to be slightly affected by the weak static and dynamic disorder in the channels and by traces of ADDA or DAAD connections for the non-centrosymmetric molecules. In order to evaluate mobility values, other ingredients to be determined are the internal reorganization energy λ_i and the free enthalpy ΔG^0 . In the case of centrosymmetric molecules inside PHTP-like channels, the ΔG^0 parameter is expected to be generally small since the only source of energetic mismatch arises from the application of an external electric field or from small local fluctuations in the host-guest interactions. In contrast, when push–pull molecules are aligned in the channels in a regular ADAD fashion, the static Coulomb interaction between the permanent dipoles is likely to introduce some energetic disorder along the channel. This has been investigated here in the case of PNA by calculating at the DFT level (with the B3LYP functional and a 6-311G* basis set) the energy of the HOMO and LUMO levels of the individual molecules in 1D arrays containing from 3 to 8 molecules, see Figure 6 (the intermolecular distance has been fixed at the van der Waals contact of 9.23 Å between the centers of mass). Figure 6c shows the energy landscape of the HOMO and LUMO levels in a system containing 8 PNA molecules. An energy gradient is clearly observed along the stack; in the case of the system containing 8 PNA units, the total variation in the HOMO and LUMO energy amounts to 1.52 eV and

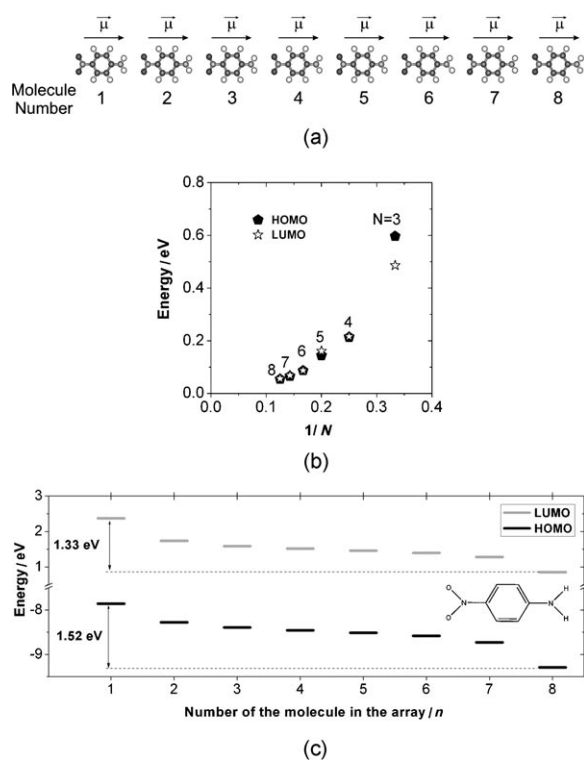


Figure 6. a) Structure of the array containing 8 PNA molecules in a head-to-tail configuration; b) energetic difference between the frontier orbitals of the central molecules in the array versus the number of molecules (N); c) Variation of the HOMO and LUMO energies of the individual molecules in a one-dimensional array containing 8 PNA molecules.

1.33 eV, respectively. The gradient is minimized in the center of the array since the central molecules have a well-balanced interaction with the surrounding positively and negatively charged sites. In contrast, there is a pronounced energy difference between the levels at the extremity of the stack due to the lack of compensation. The evolution of the energy difference between two adjacent molecules in the center of the array as a function of the number of molecules suggests that it evolves towards vanishingly small values for a macroscopic system, see Figure 6b. On the other hand, the energy gradient persists at the extremities of the channel, thus indicating that there is a priori a preferential direction for hole and electron transport along the channels (from right to left for electrons in Figure 6c and *vice versa* for holes). However, the internal field responsible for the energy gradient will be compensated by external charges when connecting the host-guest system to metallic electrodes to perform transport measurements.^[22] Accordingly, we have set ΔG^0 equal to zero in Equation (1), thus assuming that the applied electric field is weak.

The calculated internal reorganization energies (λ_i) of the compounds are given in Table 1. In PNA, the strong localization of the LUMO level over the nitro group increases the amount of local distortion and yields an internal reorganization energy larger for electrons than for holes. Table 1 also collects the mobility values at 300 K obtained from Equation (4) by inserting the transfer rate k_{hop} estimated from the various molecular parameters according to Equation (1). The calculated mobilities primarily reflect the amplitude of the corresponding transfer integrals. In the case of a perfect collinear array, the largest mobility value for holes [electrons] is obtained for PNA [PICS] and amounts to $\sim 0.4 \text{ cm}^2 \text{ V}^{-1} \text{ s}^{-1}$ [$\sim 0.2 \text{ cm}^2 \text{ V}^{-1} \text{ s}^{-1}$] for $\lambda_s = 0.2 \text{ eV}$; this represents an improvement by more than one order of magnitude compared to stilbene or oligoacenes. For the latter series, the size evolution of the mobility also reflects the trends observed for the transfer integrals, see Figure 3. This demonstrates in the present case that an array with N molecules having a molecular length L yields a higher charge carrier mobility than an array with $N/2$ molecules with a molecular length $2L$. This trend is supported by experimental measurements of electron mobility in ultra-purified molecular crystals of naphthalene^[39] and anthracene^[40] along the c axis (featuring a quasi co-linear alignment) that provide mobility values of $0.44 \text{ cm}^2 \text{ V}^{-1} \text{ s}^{-1}$ for naphthalene and $0.38 \text{ cm}^2 \text{ V}^{-1} \text{ s}^{-1}$ for anthracene. Note that a decrease in the mobility with molecular length can only be seen when dealing with rather short molecules for which the transport is described by the hopping regime. Longer conjugated chains are expected to exhibit a

Table 1. Calculated molecular parameters: internal reorganization energy (λ_i), transfer integral (t), and charge mobility (μ). λ_i is the external reorganization energy assumed to be 0.2 and 0.3 eV. The free enthalpy is set to $\Delta G^0 = 0$ to compute the mobility values.

Compound	λ_i [eV]		t [10^{-3} eV]		μ [$\text{cm}^2 \text{ V}^{-1} \text{ s}^{-1}$] $\lambda_s = 0.2 \text{ eV}$		μ [$\text{cm}^2 \text{ V}^{-1} \text{ s}^{-1}$] $\lambda_s = 0.3 \text{ eV}$	
	Holes	Electrons	Holes	Electrons	Holes	Electrons	Holes	Electrons
Stilbene	0.22	0.27	5.65	11.56	0.021	0.069	0.007	0.022
PICS	0.22	0.16	14.31	11.16	0.217	0.178	0.068	0.055
PNA	0.19	0.48	33.53	23.92	0.386	0.046	0.120	0.014
Naphthalene	0.19	0.26	1.05	14.92	0.0004	0.052	0.0001	0.016
Anthracene	0.14 ^[a]	0.20 ^[a]	0.98	9.47	0.0007	0.046	0.0002	0.014
Tetracene	0.11 ^[a]	0.16 ^[a]	0.93	6.28	0.0008	0.037	0.0003	0.011
Pentacene	0.10 ^[a]	0.13 ^[a]	0.67	4.23	0.0008	0.027	0.0003	0.008

[a] The values of λ_i for the oligoacenes were taken from ref. [34].

significant contribution of intrachain band-like transport and hence a pronounced increase in the mobility value compared to small chains.^[41] We also emphasize that the trends obtained for the series of short acenes might look different for other homologous series. In general, the optimized charge carrier mobilities often fall within the range of values from 10^{-3} to $10^{-1} \text{ cm}^2 \text{ V}^{-1} \text{ s}^{-1}$, typically considered of interest for applications in field-effect transistors or solar cells;^[38] this demonstrates the potential of host-guest systems for opto-electronic applications.

4. Conclusions

We have characterized at the quantum-chemical level the molecular parameters that determine the efficiency of charge transport along one-dimensional collinear arrays built with various organic conjugated molecules. The transfer integrals are maximized in short conjugated systems due to the reduced delocalization of the frontier electronic levels. Push-pull (donor-acceptor) systems typically favor large LCAO coefficients on the terminal atoms and prevent a good electronic communication in ADDA [DAAD] configurations for electron [hole] transport. The delocalization of the frontier orbitals should thus be well balanced to provide significant LCAO coefficients in both terminal moieties for the HOMO and LUMO levels. The collinear alignment of dipoles in nanochannels creates a significant energy offset at the ends of the channels when there is no compensation by external charges. The range of mobilities obtained by our calculations are of the same order of magnitude as that encountered in organic semiconductors currently used in opto-electronic devices. This underlines the potential of host-guest compounds for such applications.

Acknowledgements

This work was supported by the European Commission through the Human Potential Program Marie-Curie Research Training Network NANOMATCH (Grant No. MRTN-CT-2006-035884) and STREP project MODECOM (NMP-CT-2006-016434), and by the Belgian National Fund for Scientific Research. The work at Georgia Tech was primarily supported by the National Science Foundation (through the MRSEC Program under Award Number DMR-0819885). J.C., S.A., and Y.O. are research fellows of FNRS. J.G. is a Ramon y Cajal research fellow of the Spanish Ministry of Science and Innovation (MICINN), being currently a visiting researcher at the ICMol, University of Valencia, in the framework of the MICINN Consolider-Ingenio program "Molecular Nanoscience".

Keywords: donor-acceptor systems · electron transfer · host-guest chemistry · organic materials · quantum chemistry

- [1] P. J. Langley, J. Hulliger, *Chem. Soc. Rev.* **1999**, 28, 279.
- [2] G. Calzaferri, S. Huber, H. Maas, C. Minkowski, *Angew. Chem.* **2003**, 115, 3860; *Angew. Chem. Int. Ed.* **2003**, 42, 3732.
- [3] C. Gervais, T. Hertzsch, J. Hulliger, *J. Phys. Chem. B* **2005**, 109, 7961.
- [4] L. Poulsen, M. Jazdyk, J.-E. Communal, J. C. Sancho García, A. Mura, G. Bongiovanni, D. Beljonne, J. Cornil, M. Hanack, H.-J. Egelhaaf, J. Gierschner, *J. Am. Chem. Soc.* **2007**, 129, 8585.
- [5] C. Botta, G. Patrinoiu, P. Picouet, S. Yunus, J. E. Communal, F. Cordella, F. Quochi, A. Mura, G. Bongiovanni, M. Pasini, S. Destri, G. Di Silvestro, *Adv. Mater.* **2004**, 16, 1716.
- [6] J. Gierschner, L. Lüer, D. Oelkrug, E. Musluoglu, B. Behnisch, M. Hanack, *Adv. Mater.* **2000**, 12, 757.
- [7] M. Kasha, *Radiat. Res.* **1963**, 20, 55.
- [8] J. Cornil, D. A. dos Santos, X. Crispin, R. Silbey, J. L. Brédas, *J. Am. Chem. Soc.* **1998**, 120, 1289.
- [9] S. Brovelli, G. Latini, M. J. Frampton, S. O. McDonnell, F. E. Oddy, O. Fenwick, H. L. Anderson, F. Cacialli, *Nano Lett.* **2008**, 8, 4546.
- [10] T. Nguyen, J. Wu, V. Doan, B. J. Schwartz, S. H. Tolbert, *Science* **2000**, 288, 652.
- [11] G. Srinivasan, J. A. Villanueva-Garibay, K. Müller, D. Oelkrug, B. M. Medina, D. Beljonne, J. Cornil, M. Wykes, L. Viani, J. Gierschner, R. M. Alvarez, M. Jazdyk, M. Hanack, H. J. Egelhaaf, *Phys. Chem. Chem. Phys.* **2009**, 11, 4996.
- [12] L. Viani, L. Poulsen, M. Jazdyk, G. Patrinoiu, F. Cordella, A. Mura, G. Bongiovanni, C. Botta, D. Beljonne, J. Cornil, M. Hanack, H. J. Egelhaaf, J. Gierschner, *J. Phys. Chem. B* **2009**, 113, 10566.
- [13] S. Megelski, A. Lieb, M. Pauchard, A. Drechsler, S. Glaus, C. Debus, A. J. Meixner, G. Calzaferri, *J. Phys. Chem. B* **2001**, 105, 25.
- [14] M. Alohyna, B. M. Medina, L. Poulsen, J. Moreau, D. Beljonne, J. Cornil, G. Silvestro, M. Di Cerminara, F. Meinardi, R. Tubino, H. Detert, S. Schradler, H. J. Egelhaaf, C. Botta, J. Gierschner, *Adv. Funct. Mater.* **2008**, 18, 915–921.
- [15] L. Q. Dieu, A. Devaux, I. López-Duarte, M. V. Martínez-Díaz, D. Brühwiler, G. Calzaferri, T. Torres, *Chem. Commun.* **2008**, 1187.
- [16] A. J. Cadby, S. H. Tolbert, *J. Phys. Chem. B* **2005**, 109, 17879.
- [17] M. M. Yatskou, M. Meyer, S. Huber, M. Pfenniger, G. Calzaferri, *ChemPhysChem* **2003**, 4, 567.
- [18] A. Quintel, J. Hulliger, *Chem. Phys. Lett.* **1999**, 312, 567.
- [19] K. Lutkouskaya, G. Calzaferri, *J. Phys. Chem. B* **2006**, 110, 5633.
- [20] J. C. Sancho-García, J. L. Brédas, D. Beljonne, J. Cornil, R. Martínez-Alvarez, M. Hanack, L. Poulsen, J. Gierschner, H. G. Mack, H. J. Egelhaaf, D. Oelkrug, *J. Phys. Chem. B* **2005**, 109, 4872.
- [21] N. Gfeller, G. Calzaferri, *J. Phys. Chem. B* **1997**, 101, 1396.
- [22] A. Quintel, J. Hulliger, *Synth. Met.* **1999**, 107, 183.
- [23] J. L. Brédas, J. Ph. Calbert, D. A. da Silva Filho, J. Cornil, *Proc. Natl. Acad. Sci. USA* **2002**, 99, 5804.
- [24] R. A. Marcus, *Rev. Mod. Phys.* **1993**, 65, 599.
- [25] V. Coropceanu, J. Cornil, D. A. da Silva Filho, Y. Olivier, R. Silbey, J. L. Brédas, *Chem. Rev.* **2007**, 107, 926.
- [26] A. Troisi, *Adv. Mater.* **2007**, 19, 2000.
- [27] J. L. Brédas, D. Beljonne, V. Coropceanu, J. Cornil, *Chem. Rev.* **2004**, 104, 4971.
- [28] E. F. Valeev, V. Coropceanu, D. A. da Silva Filho, S. Salman, J. L. Brédas, *J. Am. Chem. Soc.* **2006**, 128, 9882.
- [29] A. Van Vooren, V. Lemaure, A. Ye, D. Beljonne, J. Cornil, *ChemPhysChem* **2007**, 8, 1240.
- [30] K. Senthilkumar, F. C. Grozema, F. M. Bickelhaupt, L. D. A. Siebbeles, *J. Chem. Phys.* **2003**, 119, 9809.
- [31] J. S. Huang, M. J. Kertesz, *J. Chem. Phys.* **2005**, 122, 1234707.
- [32] M. D. Newton, *Chem. Rev.* **1991**, 91, 767.
- [33] V. Lemaure, M. Steel, D. Beljonne, J. L. Brédas, J. Cornil, *J. Am. Chem. Soc.* **2005**, 127, 6077.
- [34] V. Coropceanu, M. Malagoli, D. A. da Silva Filho, N. E. Gruhn, T. G. Bill, J. L. Brédas, *Phys. Rev. Lett.* **2002**, 89, 275503.
- [35] Y. Olivier, V. Lemaure, J. L. Brédas, J. Cornil, *J. Phys. Chem. A* **2006**, 110, 6356.
- [36] D. H. Dunlap, P. E. Parris, V. M. Kenkre, *Phys. Rev. Lett.* **1996**, 77, 542.
- [37] V. Coropceanu, J. M. André, M. Malagoli, J. L. Brédas, *Theor. Chem. Acc.* **2003**, 110, 59.
- [38] A. R. Murphy, J. M. J. Fréchet, *Chem. Rev.* **2007**, 107, 1066.
- [39] L. B. Schein, A. R. McGhie, *Phys. Rev. B* **1979**, 20, 1631.
- [40] N. Karl, J. Marktanner, *Mol. Cryst. Liq. Cryst.* **2001**, 355, 149.
- [41] P. Prins, F. C. Grozema, J. M. Schins, S. Patil, U. Scherf, L. D. A. Siebbeles, *Phys. Rev. Lett.* **2006**, 96, 146601.

Received: November 16, 2009

Published online on March 9, 2010